Widely Tunable RF Signal Generation Using an InP/Si_3N_4 Hybrid Integrated Dual-Wavelength Optical Heterodyne Source

Robinson Guzmán, Luis González, Alberto Zarzuelo, Jessica Cesar Cuello, Muhsin Ali, Ilka Visscher, Robert Grootjans, Jörn P. Epping, Chris G. H. Roeloffzen, and Guillermo Carpintero

***Abstract*—Photonics-based techniques spearhead the generation of high-frequency signals in the millimeter-and Terahertz wave, crucial for ultrabroadband mobile wireless link development. Photonic integration is enabling to provide the photonic approach with added advantages of energy-efficiency, flexibility and scalability, in addition to signal quality. We present an optical heterodyne system based on a novel dual laser module containing two InP-Si_3N_4 hybrid lasers with intracavity wavelength selective optical filters with output optical power per laser of up to 15 dBm (31 mW), wide wavelength tuning of about 60 nm, and narrow optical linewidth below 100 kHz. To the best of our knowledge, we present for the first time the continuous-wave generation of RF frequencies over a wide tuning range from C-band (4 GHz – 8-GHz) to W-band (75 GHz – 110 GHz) achieving record low RF electrical linewidth around 108 kHz and long-term drift $<$ 12 MHz with two free-running lasers. This is the best beat-note linewidth obtained with such an integrated source in a free-runnning regime and with a wide tuning range ever reported.**

***Index Terms*—Hybrid laser, laser tuning, millimeter-waves, photonic integration.**

I. Introduction

IT IS expected that networks will utilize frequency bands in the millimeter-wave range (30 to 300 GHz) to deliver extreme link capacities and miniaturize transceivers [1]. These are key parameters to unlock the radio access densification in urban scenarios through wireless backhaul of small cells, which requires capacity increase to 10 Gbit/s over 3 km links, reaching up to 25 Gbit/s over 1 km distance at dense urban areas and hot spots.

Photonic-based RF signal generation techniques, due to their efficiency and maximum reachable frequency, have spearheaded the access to the millimeter-wave range [2]. Among the available techniques for continuous-wave (CW) signal generation, optical heterodyning has the widest frequency range, capable of generating RF frequencies in the microwave (3 GHz to 30 GHz), millimeter-wave and up into the Terahertz (300 GHz to 3 THz) range, with the potential of tuning the generated RF frequency (f_{RF}) over all these bands. Optical heterodyning is based on the simple principle of shining two optical wavelengths (λ_1, λ_2), with a frequency spacing given by the desired RF frequency, onto a photomixer (either a high-speed photodetector or photoconductor), generating at its contacts a beat-note signal at the difference frequency ($f_{\mathrm{RF}} = |\lambda_1 - \lambda_2|$). In addition to maximum frequency and tuning range, selection criteria usually include signal quality performance indicators such as frequency stability, linewidth, and spectral purity [3], which strongly depend on how the optical heterodyne source is implemented.

To date, most of the reported optical heterodyne sources rely on fiber interconnected discrete components, requiring a pair of tunable single-wavelength lasers (TSWLs), a fiber coupler, and a high-speed photodiode. Complex and costly external-cavity diode lasers with motorized resonator control have been used, providing narrow optical linewidth ($<$ 100 kHz) and tuning range in excess of 100 nm (12.5 THz). An alternative using Distributed Feedback (DFB) lasers, which is more compact and cost-effective, provided optical linewidth down to 650 kHz and tuning range of 1200 GHz, which could be increased to 2750 GHz by the proper combination of three lasers [4]. The main drawbacks of the discrete component approach are the size and cost of the resulting system as well as the poor stability of the generated signal resulting from using independent lasers with uncorrelated noise sources (affecting the RF signal phase noise) and independent thermal control units (affecting the frequency drift of the signal). Another key source for signal degradation in discrete component based optical heterodyne systems are the phase fluctuations between the two lasers due to optical path length variations in the optical fibers, introducing 10-20 dB of phase noise degradation at low frequencies [5].

Manuscript received January 27, 2021; revised March 28, 2021 and April 29, 2021; accepted May 2, 2021. Date of publication May 10, 2021; date of current version December 16, 2021. This work was supported in part by TERAWAY project that has received funding from European Union's Horizon 2020 Research and Innovation Programme under Grant 871668 and in part by the European Union's Horizon 2020 Research and Innovation Programme (Marie Slklodowska-Curie) under Grant 801538. *(Corresponding author: Robinson Guzmán.)*

Robinson Guzmán, Luis González, Alberto Zarzuelo, Jessica Cesar Cuello, Muhsin Ali, and Guillermo Carpintero are with the Grupo de Optoelectrónica y Tecnología Laser (GOTL) of Departamento de Tecnología Electrónica, Universidad Carlos III de Madrid, 28911 Madrid, Spain (e-mail: rcguzman@ing.uc3m.es; lgguerre@ing.uc3m.es; azarzuel@pa.uc3m.es; jecesarc@ing.uc3m.es; muali@ing.uc3m.es; guiller@ing.uc3m.es).

Ilka Visscher, Robert Grootjans, Jörn P. Epping, and Chris G. H. Roeloffzen are with LioniX International BV, AL 7500 Enschede, The Netherlands (e-mail: i.visscher@lionix-int.com; r.grootjans@lionix-int.com; j.p.epping@lionix-int.com; c.g.h.roeloffzen@lionix-int.com).

Color versions of one or more figures in this article are available at https://doi.org/10.1109/JLT.2021.3078508.

Digital Object Identifier 10.1109/JLT.2021.3078508

In order to solve the size, cost and performance issues, photonic integration technologies have been used to develop optical heterodyne systems [6]. Indium-Phosphide (InP) monolithic integration of two DFB lasers has been demonstrated, reducing their linewidth below 300 kHz for cavity lengths of 2500-µm, achieving RF beat note linewidths below 1-MHz for frequencies ranging from 2.5 GHz to 20 GHz [7]. With this approach, a fully integrated millimeter-wave transmitter on InP was demonstrated, including two DFB lasers, 2x2 Multimode Interference (MMI) couplers, Semiconductor Optical Amplifiers (SOAs), Electro-Absorption Modulators (EAM) and Uni-Travelling Carrier Photodiodes (UTC-PD) [8]. The wavelength tuning range of each DBF laser was about 1.5 nm ($\sim$ 188 GHz) and the optical linewidth greater than 1 MHz. The advantage of the integrated approach was demonstrated when the frequency tuning range was extended above 2 THz integrating a four DFB laser array combining standard optical element building blocks (BB) from an InP photonic integration foundry platform [9]. The DFB laser BB had an individual wavelength tuning range of 5.1 nm ($\sim$600 GHz) and optical linewidth between 6.4 MHz to 10 MHz over a broad range of biasing currents levels. The key advantage of active/passive InP photonic integration foundry platforms, capable of integrating monolithically a large number of different optical components is paid at the expense of compromising the performance of individual components [8], demonstrating the key importance of the photonic integration platform to achieve high performance levels.

Currently, hybrid photonic integrated circuits have been already considered, for having the advantage of being able to use the best substrate material to achieve the optimum level of performance for each optical component. A photonic microwave generator on a heterogeneous silicon-InP platform was demonstrated, with lasers that tune over 42 nm with less than 150 kHz linewidth, generating RF signals from 1 to 112 GHz [10]. Terahertz signal generation at 330 GHz was demonstrated using an InP/Polymer hybrid integrated optical heterodyne source, including two Distributed Bragg Grating (DBR) lasers and a Y-junction optical combiner [11]. These lasers, with a wavelength tuning range of 50 nm and optical linewidth of 2.8 MHz, were injection locked to an Optical Frequency Comb (OFC) to generate a 330 GHz beat note signal with 12 kHz linewidth. Very recently, widely tunable and 290-Hz record-low intrinsic optical linewidth lasers were demonstrated on a hybrid InP/Si_3N_4 (TriPleX) platform using thermally tunable high-Q micro-ring resonators based on the low-loss Si_3N_4 waveguides [12]. A hybrid dual-frequency laser structure based on this principle was shown to generate a microwave beat frequency near 11 GHz with record-narrow intrinsic linewidth as low as 2 kHz [13].

This paper reports RF signal generation over a wide frequency range from 5.62-GHz to 154.98 GHz beating two wavelengths generated on an InP/Si_3N_4 hybrid integrated dual laser module based on two widely tunable (about 60 nm) narrow linewidth (below 100 kHz) Micro-Ring Resonator (MRRs) Extended Cavity Lasers (ECL). To the best of our knowledge, we present for the first time the generation of RF frequencies over the entire W-band (75 GHz – 110 GHz) achieving record low RF electrical linewidth around 108 kHz and long-term drift $<$ 12 MHz with two free-running lasers.

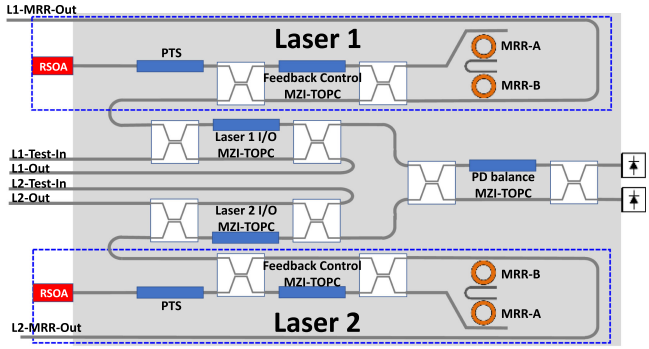

(a)

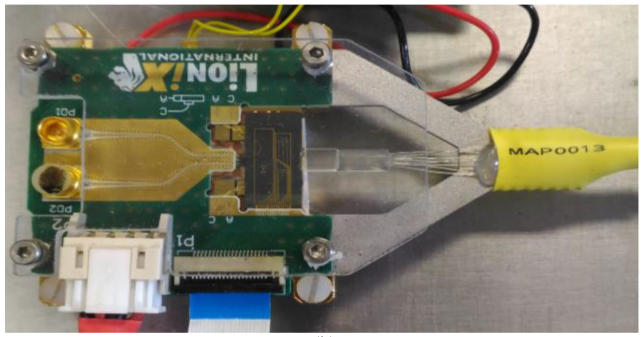

(b)

Fig. 1. (a) Schematic diagram of the hybrid optical heterodyne photonic integrated circuit (not to scale) and (b) photograph of the resulting module. RSOA: Reflective semiconductor optical amplifier, PTS: Phase tuning section, MZI-TOPC: Mach-Zehnder interferometer based thermo-optic power coupler, MRR: Micro-ring resonator, PD: Photodiode.

II. Device Description

The InP/Si_3N_4 hybrid integrated dual laser module investigated in this work is shown schematically in Fig. 1(a). As can be observed, it includes two identical laser structures, which are outlined on the figure using blue dashed boxes labeled Laser1 and Laser2 respectively. Each laser cavity is formed through hybrid integration of an InP Quantum-Well (QW) gain chip (red boxes) and a Si_3N_4 chip (gray shaded area) using butt-coupling. The InP gain chip is double-pass reflective semiconductor optical amplifier (RSOA) through high-reflective (HR) coating on the leftmost edge, which forms one of the cavity mirrors. The other mirror is an integrated mirror structure in the Si_3N_4 substrate, based on a pair of microring resonators (MRR-A and MRR-B) which provide a wavelength tunable optical feedback. The two MRRs have Free Spectral Range (FSR) around 1.6 nm (200 GHz), with slightly different radiuses to enable wavelength tuning through the Vernier effect. In between the two mirrors, the lasers include a thermally adjustable Phase Tuning Section (PTS) and a 2x2 symmetric Mach-Zehnder Interferometer based Thermo-Optic Power Coupler (MZI-TOPC) [14] which allows control of the amount of light fed back to the laser cavity. The Si_3N_4 waveguides, having a symmetric double-stripe cross section, offer a low propagation loss of about 0.1 dB/cm [15], which

allows MRRs to reach Q-factors ranging from 20000 to 200000 [12]. Each laser has an additional I/O control MZI-TOPC which allows to control the amount of the laser optical power that is directed either to the on-chip photodiodes or to an output optical fiber, L1-Out for Laser1 and L2-Out for Laser2. Finally, the on-chip photodiodes include another MZI-TOPC, which allows to control the amount of power from each laser that is directed towards each on-chip photodiode, PD1 and PD2.

A photograph of the InP/Si_3N_4 hybrid integrated dual laser module is shown in Fig. 1(b). As shown in the image, the optical waveguide access ports are coupled to single mode polarization maintaining fibers, which are terminated with an angled facet FC/APC connector to prevent undesired reflections back into the laser cavity.

III. Device Characterization

The InP-Si_3N_4 hybrid integrated dual laser module is assembled on a thermally controlled base through a Peltier thermoelectric cooler (TEC) and NTC thermistor. The module is operated at 20°C throughout all the reported measurements. The current injected on the gain section RSOAs is driven from custom battery supply current sources, to reduce the electrical noise, while the heaters in the chip, one per each Mach-Zehnder Interferometer based Thermo-Optic Power Coupler, as well as the heaters from the MRRs are driven from low-noise voltage sources, Keysight E3611.

A. Power Threshold and MZI-TOPC Characteristics

The first step is to measure the threshold current of each laser, sweeping the current injected into each RSOA from 0 mA to 30 mA, without applying any voltage to any heater. The result is that both lasers have a similar threshold current, around 10 mA. We have also measured the maximum optical output power from Laser 1 and Laser 2 at their corresponding output waveguides L1-Out and L2-Out, using a Thorlabs PM200 optical power meter. As we discussed in the previous section, the optical power at these output waveguides is controlled by the voltage applied to the heater of the corresponding I/O control MZI-TOPC. The measured output power for Laser 1 as the heater voltage is varied from 0 V to 20 V, at a fixed current level into the RSOA of 60 mA is shown in Fig. 2. The optical output power varies from about -54 dBm to 6.6 dBm at 75 V^2 (8.67 V) and 325 V^2 (18.1 V) respectively, achieving an extinction ratio of 60.6 dB. The maximum optical optical output power was achieved injecting a 250 mA forward current into the RSOA gain section, obtaining 15 dBm (31 mW).

B. Wavelength Tuning Characteristics

Once that the I/O control MZI-TOPC behavior is known, we move to analyzing the wavelength tuning characteristics. For this analysis, we set the Laser 1 and Laser 2 RSOAs bias current to 60 mA and 32 mA respectively, while driving the I/O control MZI-TOPC heater to get 0 dBm of optical power at the output waveguide, the measured and recorded optical output is registered by an Anritsu MS9740A optical spectrum analyzer with a 0.03 nm resolution.

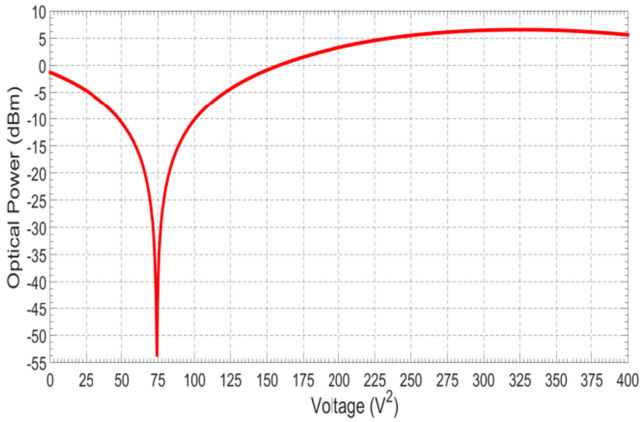

Fig. 2. Optical output power from Laser1, at 60 mA current injected into RSOA, as the I/O control MZI-TOPC heater is swept from 0 to 20 V. Voltage axis is drawn as V^2 unit as the thermal shift depends on the electrical power.

The wavelength of each laser is tuned varying the voltages applied to MRR-A and MRR-B heaters independently, sweeping the voltage of MRR-B from 0 V to 12 V for every step of MRR-A, which is also swept from 0 V to 12 V. The emission wavelength tuning that is achieve for Laser1 and Laser 2 are shown in the maps of Fig 3(a) and Fig. 3(b) respectively. As becomes evident, the initial wavelength of both lasers is 40 nm apart, with Laser 1 starting at 1551 nm and Laser 2 at 1503 nm. This difference is due to the fact that the RSOA gain chips are two different die chips, with different gain profiles. Over these maps we can define two tuning strategies for these lasers.

The first strategy, which we shall call "coarse tuning", is to tune one of the MRR through its heater bias voltage keeping the other MRR heater at a fixed bias voltage. Varying MRR-A provides horizontal travel directions along the wavelength map, while MRR-B provides vertical directions. Fig. 4(a) shows the optical spectrum shift under this coarse tuning strategy for Laser 1, fixing MRR-A at 0 V and tuning MRR-B from 0 V to 12 V in 1 V steps. The starting wavelength is 1551.105 nm, corresponding to both MRRs set to 0 V. We observe a ∼37 nm tuning range with steps of 1,6 nm (200 GHz) corresponding to the Free-Spectral-Range (FSR) of the fixed MRR. Fig. 4(b) shows that the wavelength tuning ($\Delta\lambda$) is linearly dependent on the electrical power (ΔV^2) applied to the MRR heater, with a slope 0.25 nm/V^2. The evolution towards decreasing wavelength values is confirmed in the wavelength tuning map on Fig. 3(a), along the vertical MRR-B tunning direction. Also, Fig. 4(a) allows us to appreciate a 50 dB Side-Mode Suppression Ratio (SMSR) at all wavelengths.

The second tuning strategy, which we shall call "fine tuning", is when we drive the heater bias voltage of both MRRs to travel along the simultaneous ring tuning directions. At these angled directions, we tune within the same MRR FSR, achieving smaller tuning steps and therefore, smaller tuning range. Fig. 4(c) shows the tuning of MRR-A and MRR-B with the same voltage source from 7 V to 10 V in 1 V steps presenting a shifting from 1549.75 nm to 1550.25 nm. We also find a linear

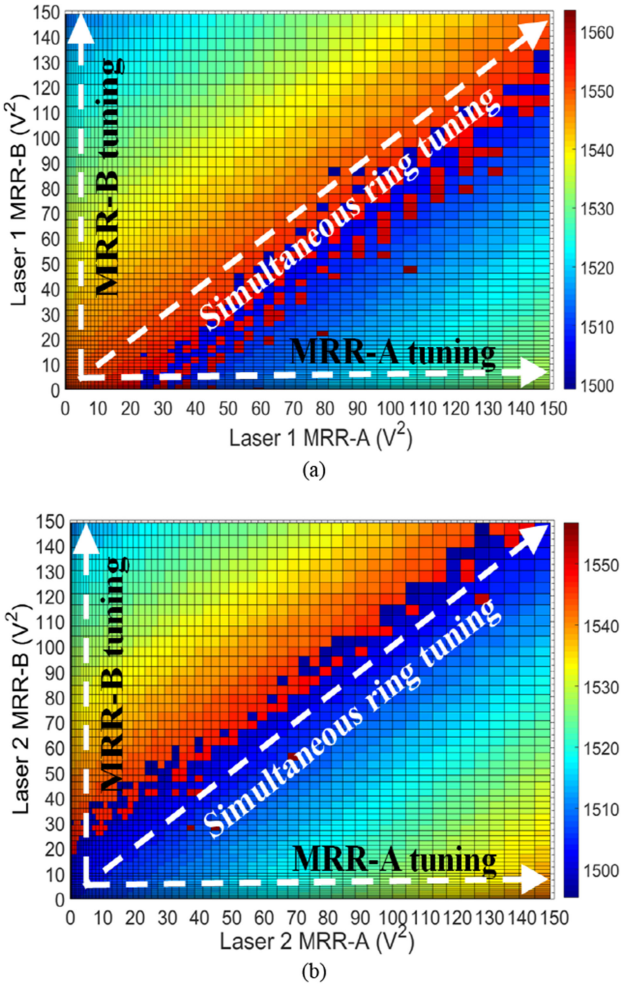

Fig. 3. Wavelength tunning map for (a) Laser 1 and (b) Laser 2 as the voltage of MRR-A and MRR-B heaters are varied, either individually (MRR-A and MRR-B routes) or simultaneously, which provide very different wavelength tuning range. Individual tuning allows wavelength tuning range beyond 50 nm for both lasers.

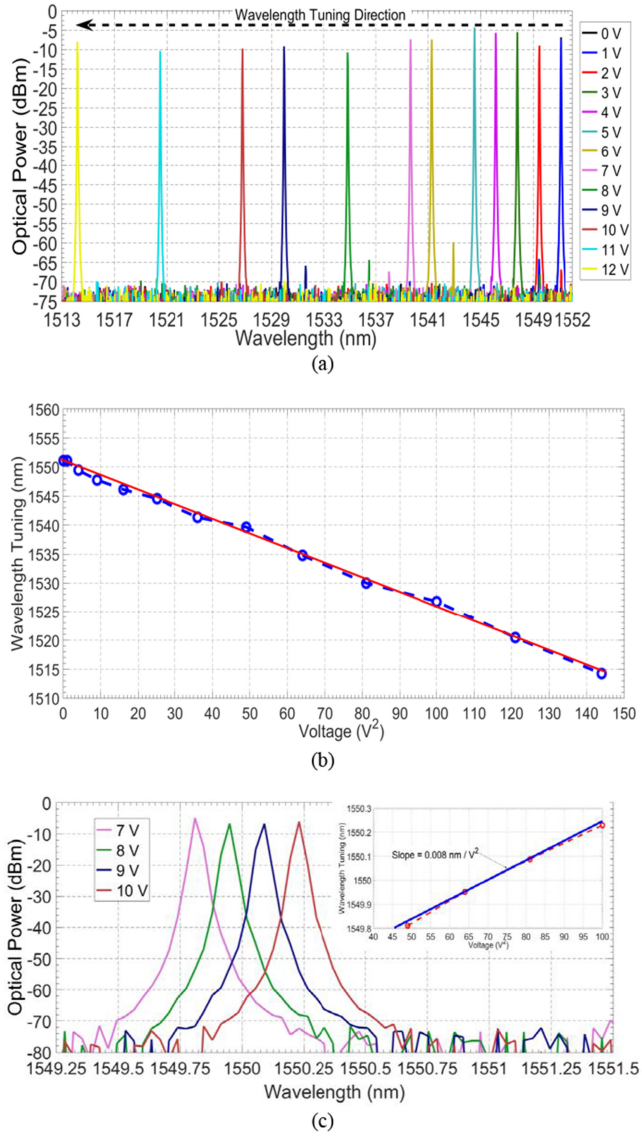

Fig. 4. Optical spectrum of Laser1 as the MRRs are varied: (a) Tuning of a single MRR (coarse tuning), MRR-A fixed at 0 V, MRR-B sweep from 0 V to 12 V, (b) coarse tuning linear wavelength trend (slope = 0.2564 nm / V^2 ($\Delta\lambda/\Delta V^2$), and (c) tuning both MRR simultaneously (fine tuning), sweeping applied voltage from 7 V to 10 V in 1V steps. Inset shows wavelength linear trend with slope of 0.008 nm / V^2.

dependence of the emission wavelength with the electrical power (voltage squared) injected into the heaters in the fine-tuning strategy, with a slope of around 0.008 nm/V^2 ($\Delta\lambda/\Delta V^2$), almost an order of magnitude smaller than with the coarse tuning. A detailed description of the emission wavelength selection and tuning mechanisms for these lasers can be found in [17], which exploits the Vernier effect using the pair of microring resonators (MRR-A and MRR-B) with slightly different FSR, providing wavelength selective optical feedback. Independent heaters on each MRR allows thermal tuning to shift the wavelength.

These two-wavelength tuning strategies are an interesting feature of these lasers to their application to millimeter-wave generation by optical heterodyning. An even more interesting characteristic of the wavelength tuning mechanism in these lasers is the extremely high repeatability, generating the same wavelength for the same combination of MRRs heater control values, even when the laser is operated at different times.

As we have shown, the two lasers start at quite different wavelengths, 50 nm (6,25 THz) apart. This is an issue for millimeter-wave generation since it is too high frequency. Instead of applying high voltages to the MRRs to get the two lasers into the millimeter-wave range (30 to 300 GHz), there is an alternative way of acting on the Feedback Control MZI-TOPC of each laser. To show this effect, we have drawn the mapping of the emission wavelength as a function of the voltage applied to the corresponding Feedback Control MZI-TOPC heater, shown in Fig. 5(a) for Laser 1 and in Fig. 5(b) for Laser 2. In this mapping, we sweep the Feedback Control MZI-TOPC heater and MRR-A wavelength tuning resonator. As becomes evident now, the emission wavelength swings between 1500 nm to 1550 nm under the voltage applied to the Feedback Control MZI-TOPC. This allows to set the two lasers in the same wavelength range.

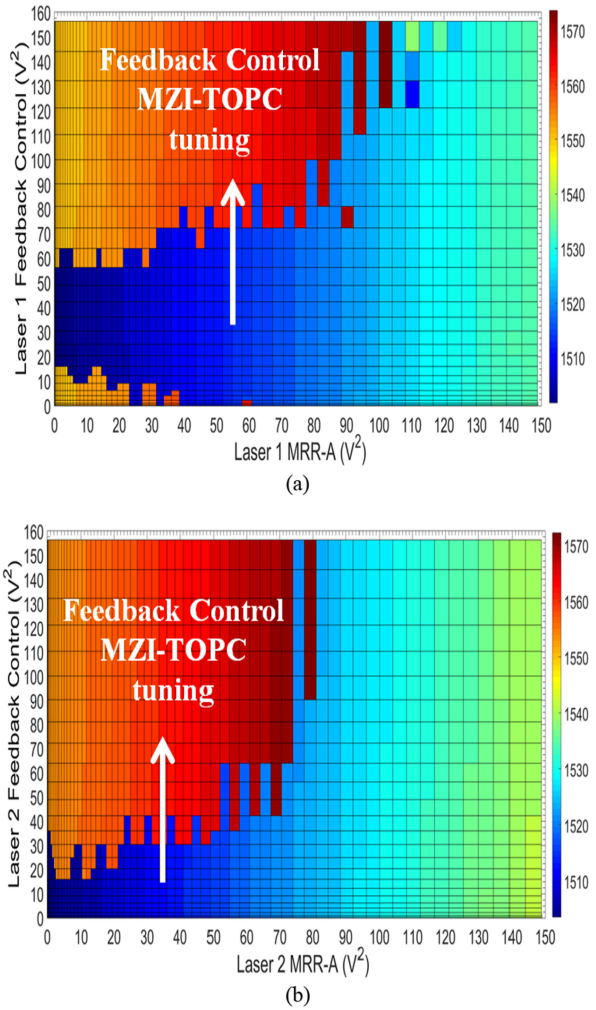

Fig. 5. Mapping of the wavelength tunning for Laser 1 (a) and Laser 2 (b) using the feedback control MZI-TOPC and MRR-A tuning ring resonator from 0 V to 12 V in 0.5 V steps.

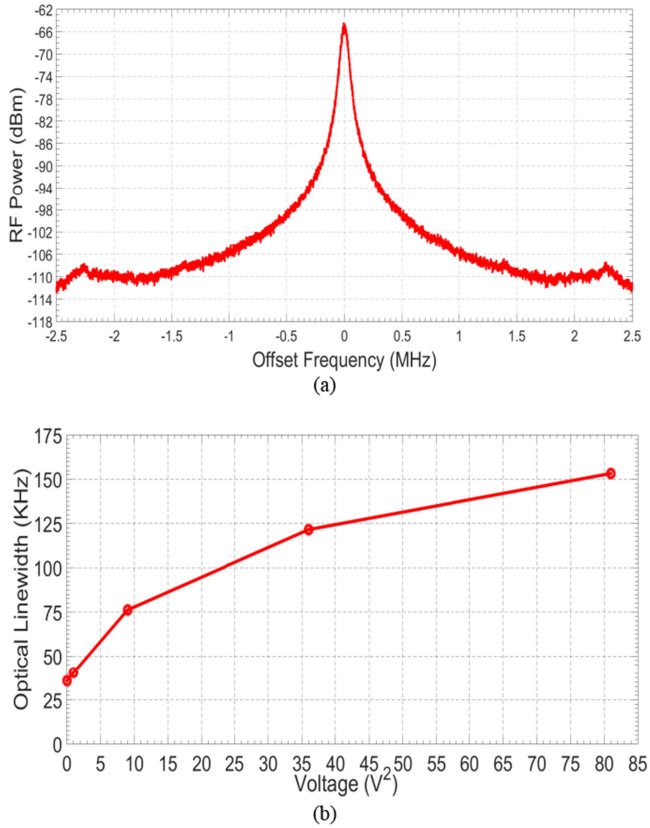

Fig. 6. (a) Self-herterodyne spectrum centered at 40 MHz with a span of 5 MHz (RBW=1 KHz, VBW=5 Hz) (b) optical linewidth of laser 1 at different values of voltage applied to both MRRs simultaneously.

C. Optical Linewidth

A key parameter for optical heterodyne millimeter-wave generation is the optical linewidth of the two wavelengths that beat together, since these determine the linewidth of the generated RF signal. We have measured the optical linewidth of the two lasers using a delayed self-heterodyne setup using a 40-MHz fibered acousto-optic modulator and a length of 6.8 km of single mode optical fiber between the two arms of the interferometer. The photodetected beat-note at 40-MHz is sent to a FSW50 electrical spectrum analyzer (ESA), on which we recorded the beat note spectrum at 40-MHz. The linewidth was extracted assuming a lorentzian shape and fitting the -10 dB level. The optical -3 dB linewidth was then assumed to be half the -3 dB linewidth of the electrical tone.

The measured results are presented in Figure 6. First, we record the self-heterodyne 40-MHz beat note of Laser 1 when the two MRRs are set to 0 V, shown in Fig. 6(a), where we observe an electrical FWHM (Full Width half Maximum) linewidth around 25 kHz. From this starting point, we start to fine tune the emission wavelength, varying the voltage applied to both MRRs simultaneously, and measure the optical linewidth at different tuning voltages. The resulting optical linewidth evolution is shown in Fig. 6(b), where we observe an increase of the linewidth with the increasing tuning voltage, remaining below 160 kHz over the entire range.

It is clear that the lasers do not reach the smallest value of 290 Hz reported previously for InP/Si_3N_4 hybrid integrated lasers [12], but the structure of the laser is different, including an on-chip wavelength combiner for the two lasers and a pair of photodiodes. Nevertheless, it is comparable to previously reported values with this technology [15] and is narrower than with other integrated alternatives [7], [8], [9], [10].

IV. Millimeter-Wave Generation

We now move to the demonstration of RF generation beating the wavelengths from the two laser integrated in the InP-Si_3N_4 hybrid integrated dual laser module operating as an integrated optical heterodyne source. It is worth to highlight that we will be operating both lasers in a free-running condition, avoiding phase-locking techniques to reduce the phase noise, aiming to determine the RF signal quality from such excellent narrow optical linewidth laser sources.

As a first step, we plot the optical wavelength tuning for both lasers in a single plot, to determine the available wavelength differences. In this case, we switch Laser 2 initial emission

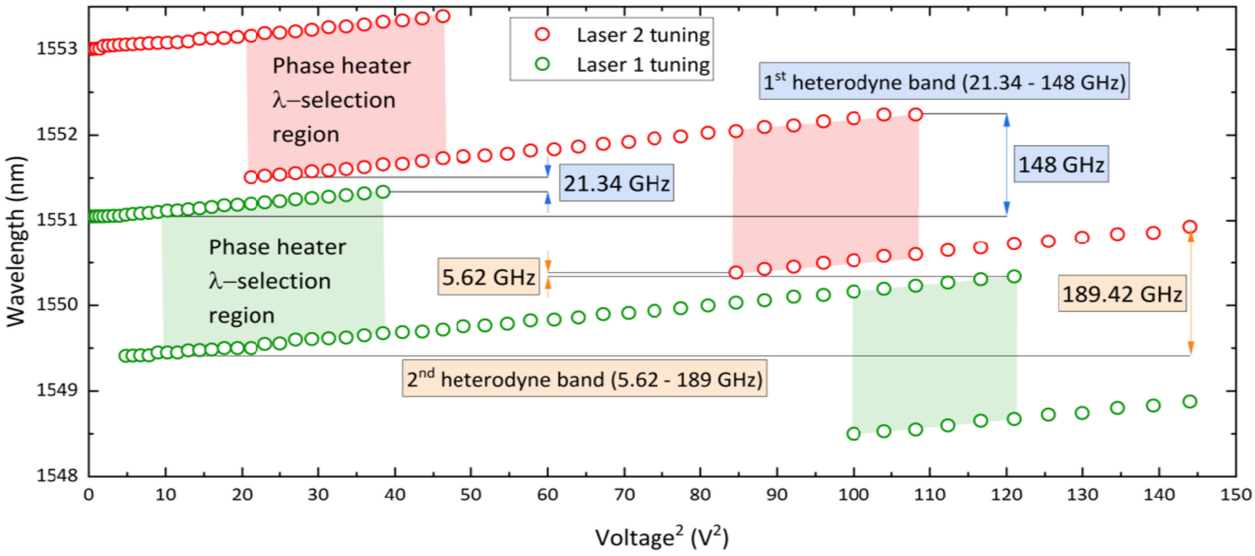

Fig. 7. Fine wavelength tuning of laser 1 (green line) and laser 2 (red line)

wavelength to 1550 nm range through the Feedback Control MZI-TOPC heater. With this action we achieve that Laser 1 and Laser 2 starting wavelength are 1551 nm and 1553 nm respectively. We then tune the emission wavelength of each laser using the fine tuning strategy, sweeping both MRRs simultaneously from 0 V to 12 V, recording their emission wavelength.

The result is shown in Fig. 7, where Laser1 is plotted with green trace and Laser 2 with a red trace. A we already mentioned, there is a linear dependence between the wavelength change and the electrical power applied to the MRR heaters. In this graph, the y-axis difference between any point in Laser 1 trace and any other point from Laser 2 trace corresponds to the wavelength difference between the two lasers, which in turn determines the RF frequency that would be generated in a photodiode. On Fig. 7 we observe that the two lasers exhibit continuously tunable ranges, at the end of which there is a wavelength jumps of 1.5 nm, corresponding to the MRR FSR.

The continuous wavelength tuning ranges of the two lasers allow us to define two optical heterodyne bands. The first one, labeled 1st heterodyne band in Fig. 7, is centered around 1551.5 nm. The minimum wavelength spacing between the two lasers in this band is 21.34 GHz, while the maximum wavelength spacing is 148 GHz. The second heterodyne band that we observe, labeled 2nd heterodyne band in Fig. 7, is centered around 1550 nm. In this second band, the minimum and maximum wavelength spacings are 5.62 GHz and 189.4 GHz respectively. These bands allow generating RF frequencies over an extremely wide tuning range covering from the RF C-band (4 GHz to 8 GHz) to the W-band (75 GHz to 100 GHz) and beyond.

Regarding the wavelength jumps at the extremes of the continuous wavelength tuning regions, these happen due shifts in the MRR resonance at which lasing happens. These lasers have two MRRs with slightly different FSR to select a single emission wavelength through the Vernier effect. These wavelength jumps correspond to a shift of the emission wavelength between adjacent MRR resonances. It is interesting to note that the jump happens over wide regions in which it is possible to select the emission wavelength of the laser between the two values. The laser actually emits in just one of the two values, which is selected with the Phase Tuning Section heater included in the structure.

Now, to analyse the quality of the generated RF signal, we select the conditions that allow us to continuously tune over the entire W-band range. We use the first heterodyne band, setting Laser 1 at its initial bias condition, with all its heaters at 0 V, fixing the emission wavelength at 1551.1 nm. The wavelength of Laser 2 is then varied using the fine tuning strategy, shifting the wavelength spacing continuously from 57 GHz to 112 GHz. Fig. 8(a) shows the two optical wavelengths, being Laser 1 fixed at 1551.1 nm and Laser 2 tuned to achieve different wavelength spacing within the W-band. Within the entire tuning range, the peak power difference between the two optical wavelengths is less than 3 dB, which was guaranteed using Laser 2 feedback control MZI-TOPC. To measure the RF frequency characteristics, we first used an external U2T XPDV4120R 100-GHz - 3dB-bandwidth High-Speed Photodiode (HS-PD) with 0.5 A/W responsivity. Laser 1 and Laser 2 optical output fibers were combined with an external PM 50:50 coupler, followed by the HS-PD with a W1 coaxial connector. The signal was measured with a Rohde & Schwarz FSW 50-GHz ESA equipped with an FS-Z110 W-band harmonic mixer, which introduces around 30 dB of conversion losses. Fig. 8(b) shows the measured electrical RF signals for the different wavelength spacings in Fig. 8(a). The varying level of the generated RF power is caused by the combined frequency response of the external mixer head and HS-PD.

To give a more detailed view of the beat signal at different frequencies, we plot in Fig. 8(c) all of them over a 30 MHz span around the peak frequency with Resolution Bandwidth, RBW = 50 kHz, and Video Bandwidth, VBW = 500 Hz. We use this data to measure the linewidth of each RF beat note signal. In Fig. 8(d) we trace the measured RF linewidth

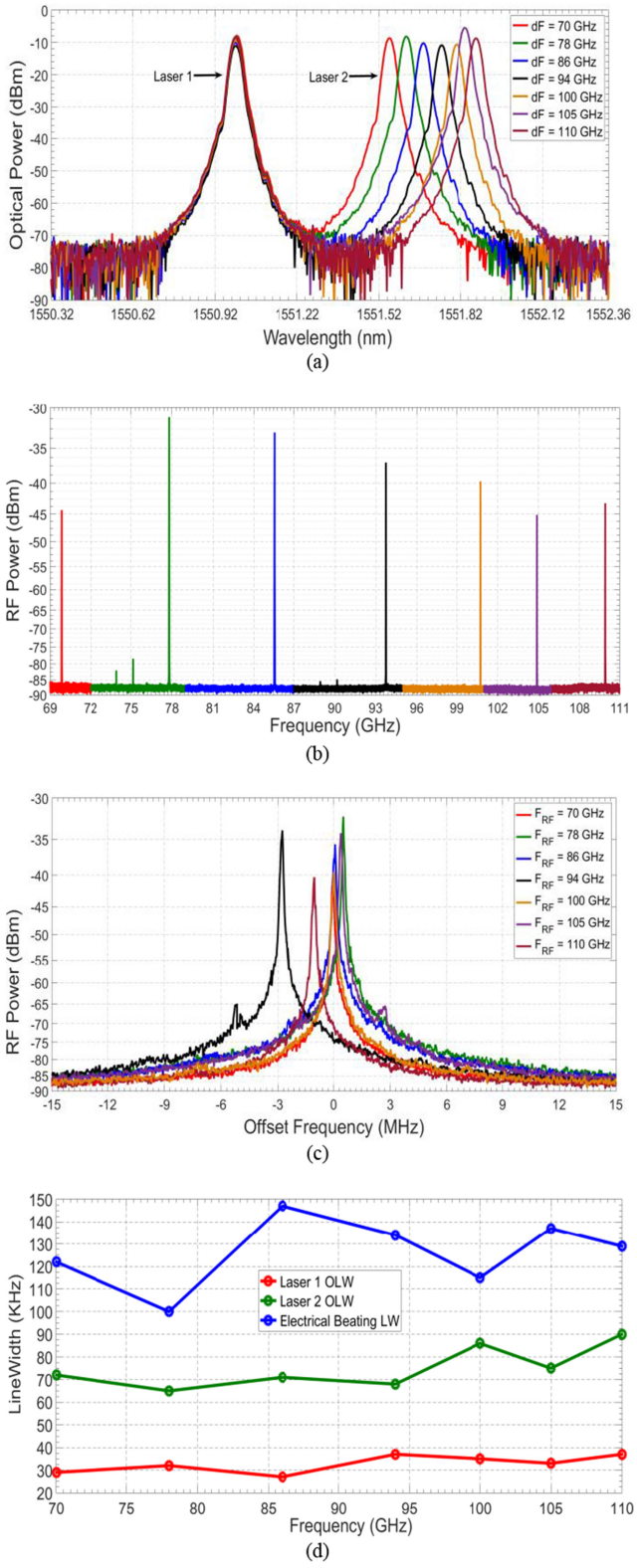

Fig. 8. (a) Superimposed optical spectrum at different wavelength spacing to generate a W-band microwave signal. (b) Superimposed electrical spectrum of the W-band microwave signal generated by the beating of the two optical modes. (c) Overlapping of each individual RF beat tone generated at the PD output. A RBW and VBW of 50 KHz and 500 Hz is used, respectively. (d) Measurement of the optcal linewidth of each single laser and the RF beat tone linewidth for each RF microwave signal generated by the dual laser.

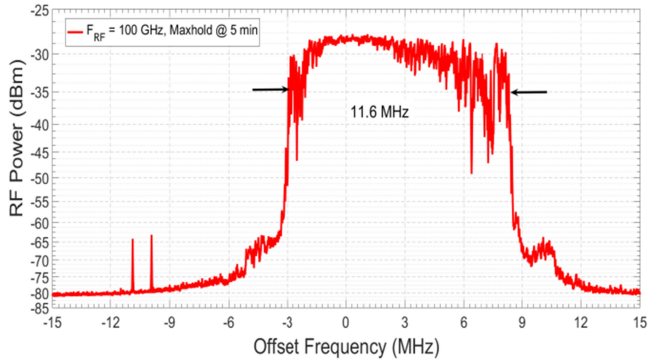

Fig. 9. Long-term drift measurement using max hold option within five minutes for an 100 GHz microwave carrier.

together with the measured optical linewidths for the two lasers generating the RF signal through optical beating. In this figure, we observe that Laser 1 has an optical linewidth ranging between 25 kHz and 40 kHz while Laser 2 ranges between 65 kHz and 90 kHz. The generated RFsignal linewidth ranges between 100 kHz and 150 kHz, which represents an order of magnitude below the current monolithic alternatives and aligned with other hybrid integrated sources, but with an extremely wide continuously tunable frequency range from 5 GHz to 150 GHz.

Lastly, we have measured the long-term drift of the generated RF signal, when the wavelength difference was set at 100 GHz. Using a max hold trace in the ESA and using a 5 minute measurement period, we achieve the trace shown in Fig. 9 which indicates a drift of about 11.8 MHz (which represents about 100 ppm), using free-running lasers.

V. Conclusion

A dual-wavelength optical heterodyne source based on InP/Si_3N_4 hybrid integration dual laser is reported. These lasers, using high-Q micro-ring resonators have an extremely wide wavelength tuning range and narrow optical linewidth. We have investigated the performance of this module as an optical heterodyne source, without any phase-locking scheme between the lasers.

An important advantage of these lasers is that present two wavelength tuning strategies, for coarse and fine tuning. With the coarse strategy, tuning one MRR heater bias voltage keeping the other fixed, wide tuning of about 60 nm range with 200 GHz steps are achieved. On the other hand, with the fine tuning, simultaneously tuning both MRRs, smaller tuning steps and range are achieved. In addition to these tuning strategies, a key feature is their extremely high repeatability, generating the same wavelength for the same combination of MRRs heater control values every time.

Beating the wavelengths generated by the two free-running lasers we have demonstrated a record-wide RF frequency tuning range from 5 GHz to 150 GHz covering a large number of RF frequency bands from C to W. Over the entire RF frequency W-band we demonstrated RF linewidths below 150 kHz and a long-term drift below 12 MHz. These characteristics turn them

into extremely good candidates for integrated optical heterodyne sources.

Currently, our system can be compared with other integrated microwaves signal generators such as Integrated Opto-Electronic Oscillators (IOEOs) [18] which has a very limited frequency tuning range of up to 20 MHz over a frequency carrier of 8.87 GHz with a phase noise of – 92 dBc/Hz @1MHz, or Electronic Integrated Circuits (EIC) oscillators which can generate high-frequency RF signal carrier using several multiplier stages to achieve the desired microwave signal. A phase noise deterioration of 20 $\log_{10}$ N (dBc/Hz) is introduced in the frequency multiplication process, where N is the multiplication factor. As a result, the phase noise performance of the multiplied signals steadily degrades with increasing oscillation frequency. The tuning range of this type of oscillator can be in the order of tens, or cents of MHz. Therefore, one of the best merits of our system is that it has a broad tuning range for high-frequency RF microwave signal generation from a few units of GHz to above 300 GHz. Another characteristic is that both the phase noise and the electrical linewidth can be improved using a phase-locking technique.

REFERENCES

[1] "Future Network Trends" Ericsson Technology Review Sep. 2020 [Online]. Available: https://www.ericsson.com/en/reports-and-papers/ericsson-technology-review/articles/technology-trends-2020#trend4

[2] T. Nagatsuma and G. Carpintero, "Recent progress and future prospect of photonics-enabled terahertz communications research," *IEICE Trans. Electron.*, vol. E98.C, no. 12, pp. 1060–1070, 2015.

[3] B. Leone *et al.*, "Optical far-IR wave generation - an ESA review study," in *Proc. 3rd ESA Workshop Millimetre Wave Technol. Appl.*, 2003

[4] A.J. Deninger *et al.*, "2.75 THz tuning with a triple-DFB laser system at 1550 nm and InGaAs photomixers," *J Infrared Milli Terahz Waves*, vol. 36, pp. 269–277, 2015.

[5] T. Nagatsuma, H. Ito, and K. Iwatsuki, "Generation of low-phase noise and frequency-tunable millimeter-/terahertz-waves using optical heterodyning techniques with UTC-PD," in *Proc. 36 Eur. Microw. Conf.*, 2006.

[6] D. Marpaung, J. Yao, and J. Capmany, "Integrated microwave photonics," *Nature Photon.*, vol. 13, pp. 80–90, 2019.

[7] F. V. Dijk, A. Accard, A. Enard, O. Drisse, D. Make, and F. Lelarge, "Monolithic dual wavelength DFB lasers for narrow linewidth heterodyne beat-note generation," in *Proc. Int. Topical Meeting Microw. Photon.*, 2011, pp. 73–76,

[8] F. V. Dijk *et al.*, "Integrated InP heterodyne millimeterwave transmitter," *IEEE Photon. Technol. Lett.*, vol. 26, no. 10, pp. 965–968, May 2014.

[9] M. Sun *et al.*, "Integrated four-wavelength DFB diode laser array for continuous-wave THZ generation," *IEEE Photon. J.*, vol. 8, no. 4, pp. 1–8, Aug. 2016.

[10] J. Hulme *et al.*, "Fully integrated microwave frequency synthesizer on heterogeneous silicon-iii/v," *Opt. Exp.*, vol. 25, no. 3, pp. 2422–2431, 2017.

[11] G. Carpintero, S. Hisatake, D. de-Felipe, R.C. Guzman, T. Nagatsuma, and N. Keil, "Wireless data transmission at terahertz carrier waves generated from a hybrid In Polymer dual tunable dbr laser photonic integrated circuit," *Nature Sci. Rep.*, vol. 8, 2018.

[12] Y. Fan *et al.*, "290 Hz intrinsic linewidth from an integrated optical chip-based widely tunable InP-Si3N4 hybrid laser," in *Proc. Conf. Lasers Electro-Opt.*, 2017, Paper. JTh5C.9.

[13] J. Mak *et al.*, "High-purity microwave generation using a dual-frequency hybrid integrated semiconductor-dielectric waveguide laser," 2020. [Online]. Available: https://arxiv.org/abs/2012.07533

[14] C.G.H. Roeloffzen *et al.*, "Silicon nitride microwave photonic circuits," *Opt. Exp.*, vol. 21, pp. 22937–22961, 2013.

[15] K. Wörhoff, R. G. Heideman, A. Leinse, and M. Hoekman, "TriPleX: A versatile dielectric photonic platform," *Adv. Opt. Technol.*, vol. 4, pp. 189–207, 2015.

[16] R. Oldenbeuving, E. J. Klein, H. L. Offerhaus, C. J. Lee, H. Song, and K. J. Boller, "25 kHz narrow spectral bandwidth of a wavelength tunable diode laser with a short waveguide-based external cavity," *Laser Phys. Lett.*, vol. 10, no. 1, 2013, Art. no. 015804.

[17] J. Epping *et al.*, "Hybrid integrated silicon nitride lasers, SPIE 2020," *Phys. Simul. Optoelectron. Devices XXVIII*, vol. 11724, 2020, Art. no. 112741L.

[18] J. Tang *et al.*, "Integrated optoelectronic oscillator," *Opt. Exp.*, vol. 26, no. 9, pp. 12257–12265, 2018.